

Full paper

Flexible fiber-based hybrid nanogenerator for biomechanical energy harvesting and physiological monitoring



Xuexian Chen^{a,b}, Yu Song^a, Zongming Su^a, Haotian Chen^b, Xiaoliang Cheng^a, Jinxin Zhang^a, Mengdi Han^a, Haixia Zhang^{a,b,*}

^a National Key Lab of Micro/Nano Fabrication Technology, Peking University, Beijing 100871, China

^b Academy for Advanced Interdisciplinary Studies, Peking University, Beijing 100871, China

Peking University

ARTICLE INFO

ABSTRACT

Keywords:

Hybrid nanogenerator
Piezoelectric
Triboelectric
Electrospinning
Healthcare monitoring

With the rapid development of wearable electronics like artificial e-skins and smart patch, harvesting biomechanical energy and realizing self-powered sensing are of essential importance for achieving sustainable and efficient function of the system. Here we report a flexible hybrid device that can be conformally attached on soft surface like human skin to harvest diversity touch energies based on electrospun nanofiber mat. Facilitated by the working mechanisms of triboelectric and piezoelectric, the device can generate maximum peak power up to $84 \mu\text{W}/\text{cm}^2$ and $0.11 \mu\text{W}/\text{cm}^2$ for the TENG and PENG part when stimulated by a compressive stress, which can enhance the energy harvesting efficiency and expand its application areas. By virtue of the high sensitivity of the piezoelectric nanomaterial, the device can also be attached on different parts of body for real-time monitoring the human physiological signals such as respiratory information and radial artery pulse, which shows potential value in self-powered e-skins and healthcare monitoring systems.

1. Introduction

Flexible and wearable electronics, including artificial electronic skins, wearable light-emitting diodes, health monitoring and motion tracking, are rapidly rising fields in today's technologies [1–6]. Although significant progress has been made in increasing the capacity of batteries and reducing the power consumption of the devices, these systems still need rigid lithium ion batteries (LIBs) with frequent replacement or charging process, which greatly limits their application areas and brings inconvenience [7]. One of the promising solutions is to scavenging energy from living environments, such as the solar energy, wind energy and mechanical energy [8–12]. Among them, harvesting mechanical energy from body motion is a feasible choice for powering portable and wearable electronics since it can be generated continuously without environment restriction [13–15]. To achieve this, biocompatible and flexible are the necessary prerequisites for wearable devices.

To date, several kinds of wearable flexible generators based on piezoelectric and triboelectric effects have been demonstrated for different body motion energy harvesting, such as textile-based triboelectric nanogenerators (TENGs) for power generation from the friction of clothes and piezoelectric nanogenerators (PENGs) for energy conversion when torsion head, bending arms and blinking, etc [16–

21]. TENGs have the advantages of low cost, easy fabrication, light weight, high efficiency and a wide choice of materials, which can be easily integrated with any surface to harvest the contact-separation energy [22–24]. However, relative displacement is required between the two friction layers for effective electric output, that is, when the harvester is continuously touched, TENG will out of function. In contrary, PENGs by employing piezoelectric materials like ZnO NWs [25], lead zirconate titanate (PZT) [26], prestigious PVDF and its copolymers can convert mechanical energy into electricity from tiny deformations [27], especially, poly(vinylidene fluoride-co-trifluoroethylene) (P(VDF-TrFE)) based piezoelectric generator was widely used owing to its large d_{33} value, low weight, flexibility and easy synthesis procedure [28–30]. In order to increase the energy conversion efficiency of the energy harvesting devices, some hybrid nanogenerators incorporating these two effects have been promoted [31–33]. However, the complex and stereo structure design make the device can only be mounted on some specific positions and cannot be widely used beyond the whole body, which restricts its application range. Therefore, a flexible and universal energy harvester with significant simplified structure and enhanced conversion efficiency is highly desired for harvesting mechanical energy from soft surfaces like human body.

To achieve excellent flexibility, all the components of the generator are required to sustain frequent random bent, including the electrode.

* Corresponding author at: National Key Lab of Micro/Nano Fabrication Technology, Peking University, Beijing 100871, China.
E-mail address: zhang-alice@pku.edu.cn (H. Zhang).

Electrospinning is a powerful technique used to produce continuous nano-sized one-dimensional structures from liquid sources of polymers. The fibers are typically collected in the form of a non-woven net, which can be used in a wide range of applications, including electrode, filters, and tissue engineering [34–36]. In particular, the strong electric field employed in the electrospinning process can induce polarization of the piezoelectric material and the electrospun nanofiber mat can be used as templates to create a continuously connected two-dimensional network of conductive nanomaterials without agglomeration [37–39].

Here in, we demonstrate a flexible film-structured hybrid nano-generator (NG) for harvesting the touch energy on soft surface based on the electrospun nanofiber mat. The whole structure integrated conductive nanomaterials coated nanofibers as electrodes, P(VDF-TrFE) nanofibers as a piezoelectric function layer and polydimethylsiloxane (PDMS) as protective cover and the friction layer. By integrating single-electrode TENG and fiber-based PENG vertically together, the device can generate electricity not only during the contact-separation process but also the continuous deformation process. Once stimulated by a compressive stress, the 2.5 cm × 3 cm hybrid NG produces maximum peak power up to 630 μW and 0.82 μW for the TENG and PENG part, respectively. The device can be excited by the simple deformation and the triboelectric charges on the top surface have a positive influence on the piezoelectric output. Besides, under the bent-recover deformation, the PENG part can also generate electric output. The hybrid NG can be conveniently attached on any soft surface to harvest mechanical energy, such as bodily contact and deformation of the sponge on chair. Furthermore, by virtue of the high sensitivity of the piezoelectric nanofibers, the hybrid NG was demonstrated as a self-powered active sensor to quantitatively monitoring human physiological signals, indicating its promising applications in smart healthcare monitoring systems and artificial electronic skins.

2. Experiment

2.1. Fabrication of flexible PENG

The fabrication of the whole device can be divided into two parts, the PENG part and TENG part, which both involved in the electrospinning process and packing of PDMS. Firstly, P(VDF-TrFE) composites solution was prepared by dissolving P(VDF-TrFE) power (solvey, 75/25 wt%) into the mixture of Dimethyl Formamid (DMF) and acetone with a ratio of 2:3 at the concentration of 15%. After stirring with magnetic spinor for 3 h, electrospinning was carried out to create piezoelectric membrane. This was done by using aluminum foil as a collector at 18 kV, a flow rate of 1 ml per hour and a tip-collector distance of 15 cm. After evaporating any remaining solvent, the resultant electrospun fiber mat was annealed at the temperature of 80 °C for 2 h and then polarized at an electric field intensity of 12.5 V/μm to help the P(VDF-TrFE) transform to β-phase and further enhance the piezoelectric performance.

To get electrospinning solution of flexible electrode, thermoplastics polyurethane (PU) particle was dissolved by dimethyl formamide/tetrahydrofuran (DMF/THF, 2:3) mixture with a weight ratio of 13% and stirred for 2 h until the solution became homogenous. The electrospinning process was conducted with a high voltage of 8 kV, 7.5 cm collecting distance and a flow rate of 1.5 ml/h. Then the as-spun PU nanofiber mat was used as a template to absorbing silver nanowires (AgNWs) with concentration of 5 mg/ml and then conductive carbon nanotube (CNT, 1 mg/ml) with length of 10–30 μm through drop and drying process. After repeating this process for several times, the PU nanofibers was coated with CNTs & AgNWs and became conductive. The flexible PENG was fabricated by sandwiching two fiber-based electrode and a P(VDF-TrFE) nanofiber mat together and then coated with PDMS solution, which was prepared by mixing the elastomer and cross-linker (Sylgard 184, Two corning) in a ratio of 10:1 (w/w) and being degassed. Then the PDMS is cured at a temperature of 80 °C for 1 h.

2.2. Fabrication of single-electrode TENG

The micro-patterned PDMS was formed by duplicating the pattern on Si wafer. Firstly, PDMS solution was spin-coated on the Si wafer with inverted pyramid structure. When the PDMS was partially cured, one piece of electrode was coated on it and peeled off with PDMS together after it was cured at 80 °C for 1 h.

Finally, the flexible PENG and TENG parts were bonded together and encapsulated through PDMS.

2.3. Measurement system

The bottom of the hybrid NG was fixed to a certain surface and the top was triggered by a vibration plate to generate periodic deformation of the device. The output current of the device was measured by a low-noise current preamplifier (Stanford Research SR570) and all the signals were recorded and displayed through a digital oscilloscope (Agilent DSO-X 2014A).

3. Results and discussion

Fig. 1a displays a photograph of the as-fabricated flexible hybrid NG that has a dimension of 2.5 cm × 3 cm. Owing to the thin-film structure and flexibility of the device, it can be conformally attached onto a balloon and easily deforms under the gently press of finger. Fig. 1b shows the detailed schematic diagram of the device with a PENG and a single-electrode TENG attached in vertical, presenting a multi-layer structure. The PENG and TENG parts are separated by a PDMS isolation layer to generate piezoelectric and triboelectric outputs individually, which is essential for guaranteeing the high output of the TENG part. The P(VDF-TrFE) and polyurethane nanocomposites were spun into nanofiber mats via electrospinning, working as piezoelectric membrane and electrodes template, respectively. The roughness of the as-spun nanofiber mat can increase the contact area between the electrode and piezoelectric layer, thereby reducing contact resistance and benefits for the derivation of piezoelectric output [40]. PDMS encapsulation layer is utilized to prevent nanofibers from suffering damage caused by direct contact with a load. The top surface of the encapsulation and friction layer is micro-fabricated into inverse-pyramid to increase the friction area and decrease the viscosity of PDMS. The complete fabrication process is schematically illustrated in Supporting Fig. S1. The SEM images of the as-spun P(VDF-TrFE) nanofiber mat and micro-patterned PDMS layer are shown in Fig. 1c and d, presenting non-woven and pyramid structures, respectively.

The flexible hybrid structure design enables the device to harvest energy on a soft surface through triboelectric and piezoelectric individually and thus increasing energy harvesting efficiency, as depicted in Fig. 1e. When a soft object is pressed, deformation on the surface will be generated intrinsically. The TENG part on the top can generate electric output when device contacts and separates with other objects and the PENG part begins to function during the deformation and recover process of soft body, because a TENG need a contact-separation process of the tribo-charges to work while the PENG only function when deformation is generated.

Since the hybrid NG is designed to harvest energy on the soft surface, flexibility is one of necessary properties of the whole structure, especially for the electrode, which is critical important for the derivation of the electric signal. In our device, non-woven structured PU nanofiber mat and the composite of conductive CNTs & AgNWs are adopted to forming flexible electrodes. To investigate the mechanical bending characteristic of the conductive fiber mat, we measured its resistance under different bending angle: $-180 \rightarrow -90 \rightarrow 0 \rightarrow 90 \rightarrow 180^\circ$. As seen from Fig. 1f, the resistance decreases when bending direction is inward and reaches a lowest value of 70 Ω between the diagonal line. This is because that the bending deformation will cause the stretch and squeeze on the electrode surface and thus the

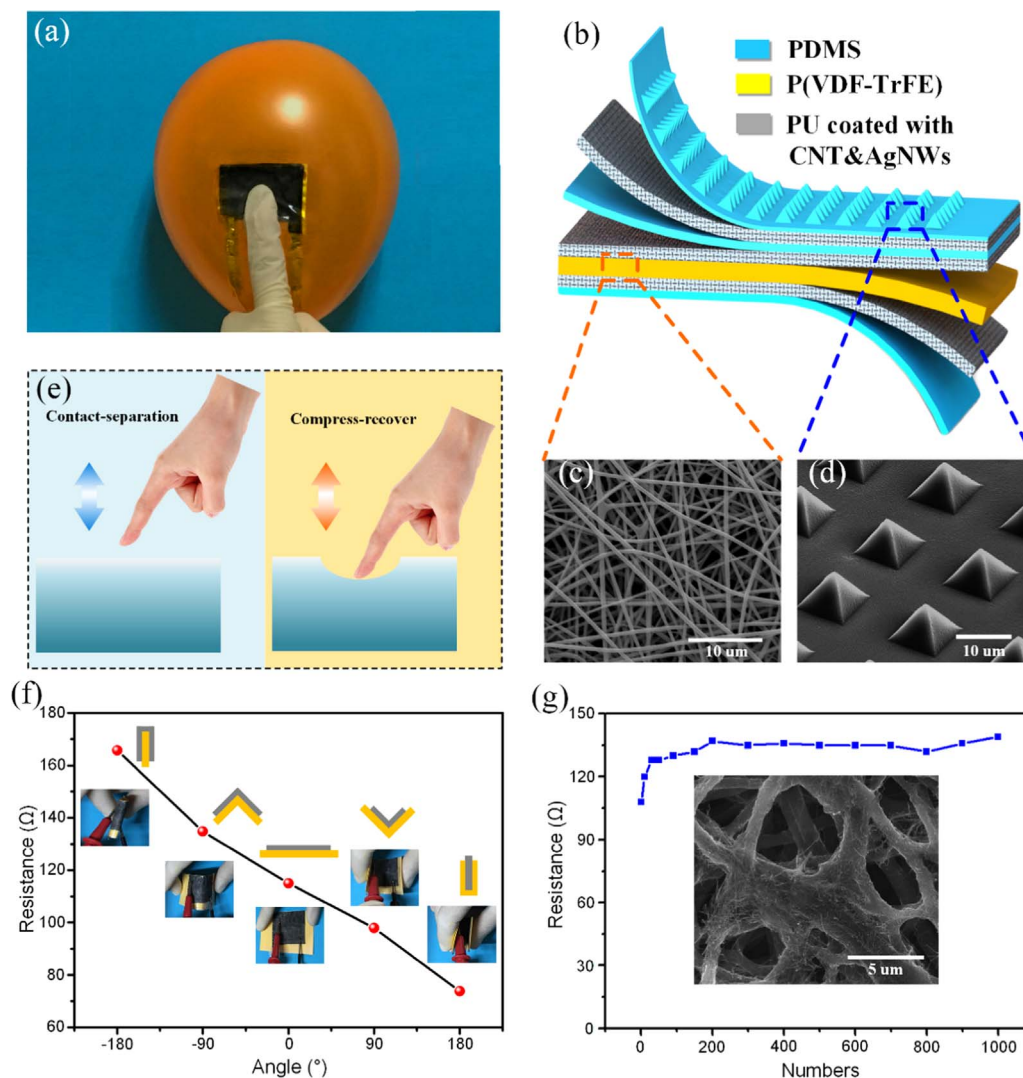


Fig. 1. Overview of the hybrid NG. (a) Photo of the device attached on the surface of a balloon. (b) Schematic diagram of the device. (c) SEM image of the electrospun P(VDF-TrFE) nanofiber mat. (d) SEM image of the pyramid structure of PDMS. (e) Two mechanical processes when a soft body is presses. (f) Conductivity measurement of the PU fiber based electrode under different bend angle. The insets shows the bend state of the electrode. (g) Stability test of the electrode under fold/unfold deformation. The inset is the SEM image of the fiber-based electrode.

realignment of the nanofibers. It worth noting that even when the electrode is folded outward completely, the resistance maintains less than 170Ω , exhibiting excellent conductive property. The inset pictures show the measurement method of the electrode. To further verify the robustness of the electrode under deformation situation, resistance change was measured through continuously repeated bend of -180° folding/unfolding for 1000 cycles, which indicates that the electrode is highly repeatable and stable (Fig. 1g). The inset picture shows the SEM image of the electrode. As can be seen, MWCNTs & AgNWs are wrapping along the PU nanofibers, thus forming a complex conductive network.

3.1. Working principle

Fig. 2a demonstrate the working mechanism of the device harvesting mechanical energy on the soft surface. As mentioned before, when the soft object is pressed, two processes will happen sequentially: the contact-separation process on the surface and the deformation-recovering process on the soft body. The TENG can only work effectively during the contact-separation process where the relative displacement happens between the friction couple. The PENG will function during the deformation-recover process. In one working cycle, the four

processes will happen continuously: contact, deformation, recovering and separation. For the TENG part, since PDMS has a strong ability of gaining electrons, objects such as cloth and hand would lose electrons and positively charged on the surface when contacts with it.

In the “contact” process, positive charges on the hand will influence the distribution of electric field on TENG electrode and drive positive charges to flow from electrode to the ground. During this process, no deformation is generated and thus there is no potential difference on piezoelectric material surface. However, the triboelectric charges can also lead to electrostatic induction on the PENG electrode and thus leading to electric output on PENG electrodes, showing by the dashed line on the Fig. 2a <i>. After hand completely contacts with the device, tribo-charges on the friction couple coincide and the TENG reach electrostatic equilibrium state. As the object is continuously pressed, the process goes into the “deformation” stage (Fig. 2a <ii>). In this stage, the deformation of device will lead to the polarization of the piezoelectric material and thus generating a piezoelectric voltage. If the device is attached on a hard surface, the deformation of piezoelectric material is mainly focus on the change of thickness and thus the PEGN works at d_{33} mode. If the device is placed on a soft object, like skin and sponge, the deformation is mainly due to the bent of the PVDF film, therefore, the PENG works at d_{31} mode. Similarly, this piezo-

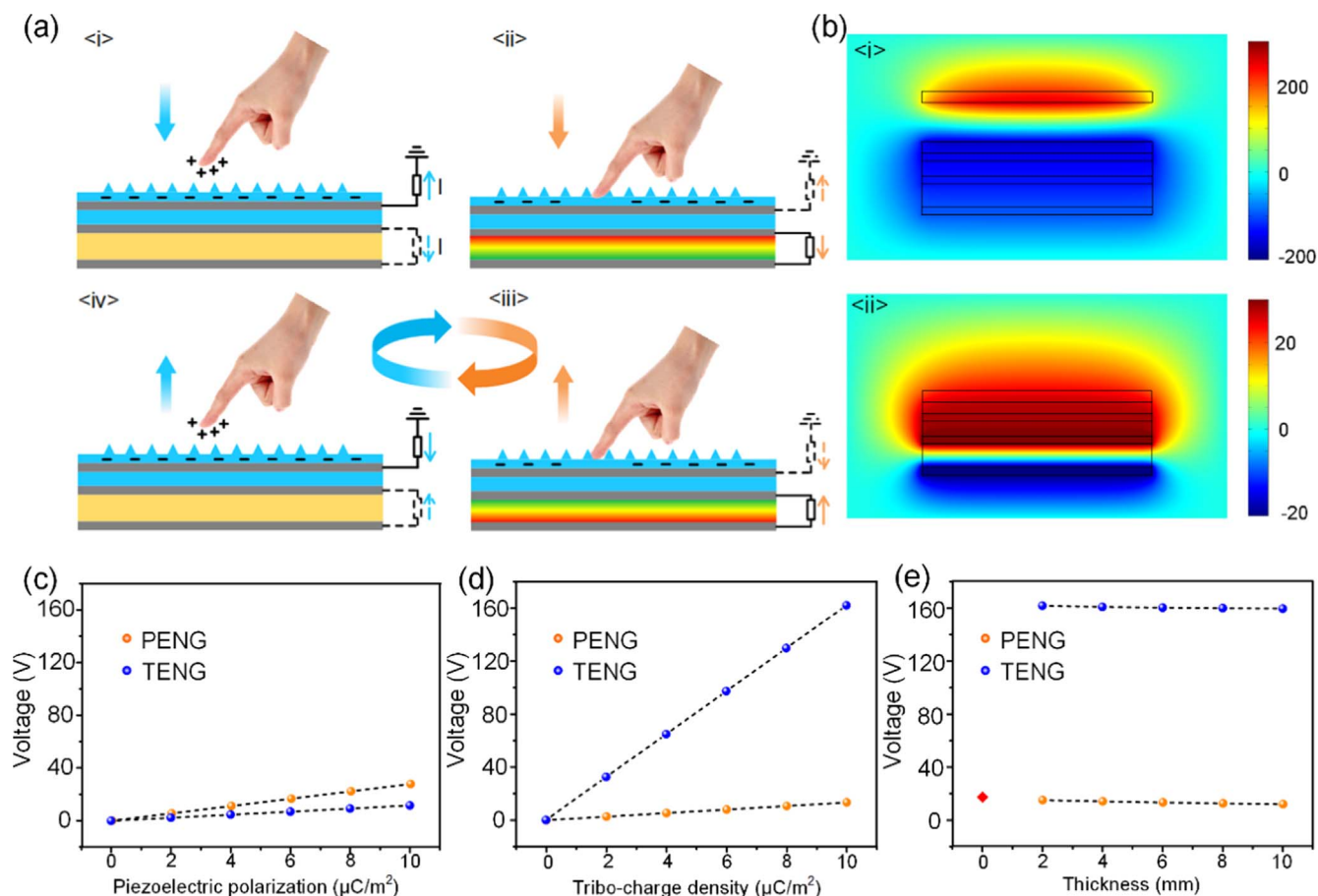


Fig. 2. Working mechanism and the simulation output of the hybrid NG. (a) Working mechanism. (b) Finite simulation indicating the potential distribution of two mechanism processes. The simulated outputs of the device under the influence of (c) piezoelectric polarization (d) tribo-charge density and (e) the thickness of the isolation layer. The red dot corresponds to the output of the device without isolation layer.

electric potential will have a little influence on the TENG electrode. After that, the hand is to leave from the device and the PENG is going to recover to its initial state, leading to reverse potential difference on it. This is the “recover” stage of the whole process, as shown in Fig. 2a <i>< iii ></i>. In this stage, the hand still fully contacts with the device and there is no triboelectric output. Then the hand deviates from the device, the center of positive and negative tribo-charges separate again and reversed triboelectric output is generated (Fig. 2a <i>< iv ></i>). Therefore, during one cycle, the TENG part will function at the first contact and last separate process while the PENG part produces output during the change of pressure. Besides, the piezoelectric film has two working mechanisms, the d_{31} mode and the d_{33} mode, which are suitable for harvesting energy on soft and hard surface through bend-recover and contact-separation process, respectively.

3.2. Output characterization

To illustrate the influence of triboelectric charges and piezoelectric potential on the output of two parts, finite-element simulation (FEM) via COMSOL Multiphysics Software was employed to simulate the electric potential distribution of the device (Fig. 2b). At the separate state, only triboelectric charges establish an electric field in the space, thus electrostatically induced positive and negative charges will accumulate on the TENG and PENG electrodes (Fig. 2b <i>< i ></i>). When the device is pressed, the centers of positive and negative tribo-charges overlap and only the piezoelectric potential exist in the space (Fig. 2b <i>< ii ></i>). Therefore, the output of the device mainly depends on the triboelectric charge density on the friction couple and the polarization intensity of the piezoelectric material. Moreover, the output of TENG

and PENG will influence each other through electrostatic induction, the polarization direction of the PENG is critical for the output enhancement of PENG. To verify this, the potential difference changes between PENG electrodes are calculated by the simulation, as shown in Fig S2a and S2b. The enhancement of piezoelectricity is also proved by experimental measurement. First, the output of PEGN is measured by forward and reverse connection. As shown in Fig. S2c, the output waveform inverts as the changing of electrode connection, verifying it is generated by the piezoelectric potential other than electrostatic induction of the electrode. Then, the output of PENG under the influence of triboelectric charges with forward and reverse polarization is investigated. For the forward polarization direction, the output voltage of PENG is enhanced from 18.3 V to 57.1 V, while the value is reduced to 13.3 V when the polarization direction is inverted. The value for the current shows the same trend. Detailed time domain output voltages are shown in Figs. S2e and 2f. This is because that the triboelectric charges on the friction layers have an electrostatic influence on the output of PENG.

Under the right polarization direction, we also investigate the influence of piezoelectric polarization, tribo-charge density and the thickness of dielectric layer on the output of the device through simulation. As seen in Fig. 2c, with the increase of the piezoelectric polarization intensity, the output for both parts have an enhancement trend. The variation tendency for the tribo-charge density shows the same trend. Therefore, it is necessary to conduct post polarization process for the P(VDF-TrFE) nanofiber mat to enhance its polarization intensity and add micro-pattern on the top surface of PDMS to increase the surface tribo-charge density, which both benefit for the enhancement of both parts. Although reducing the thickness of the isolation

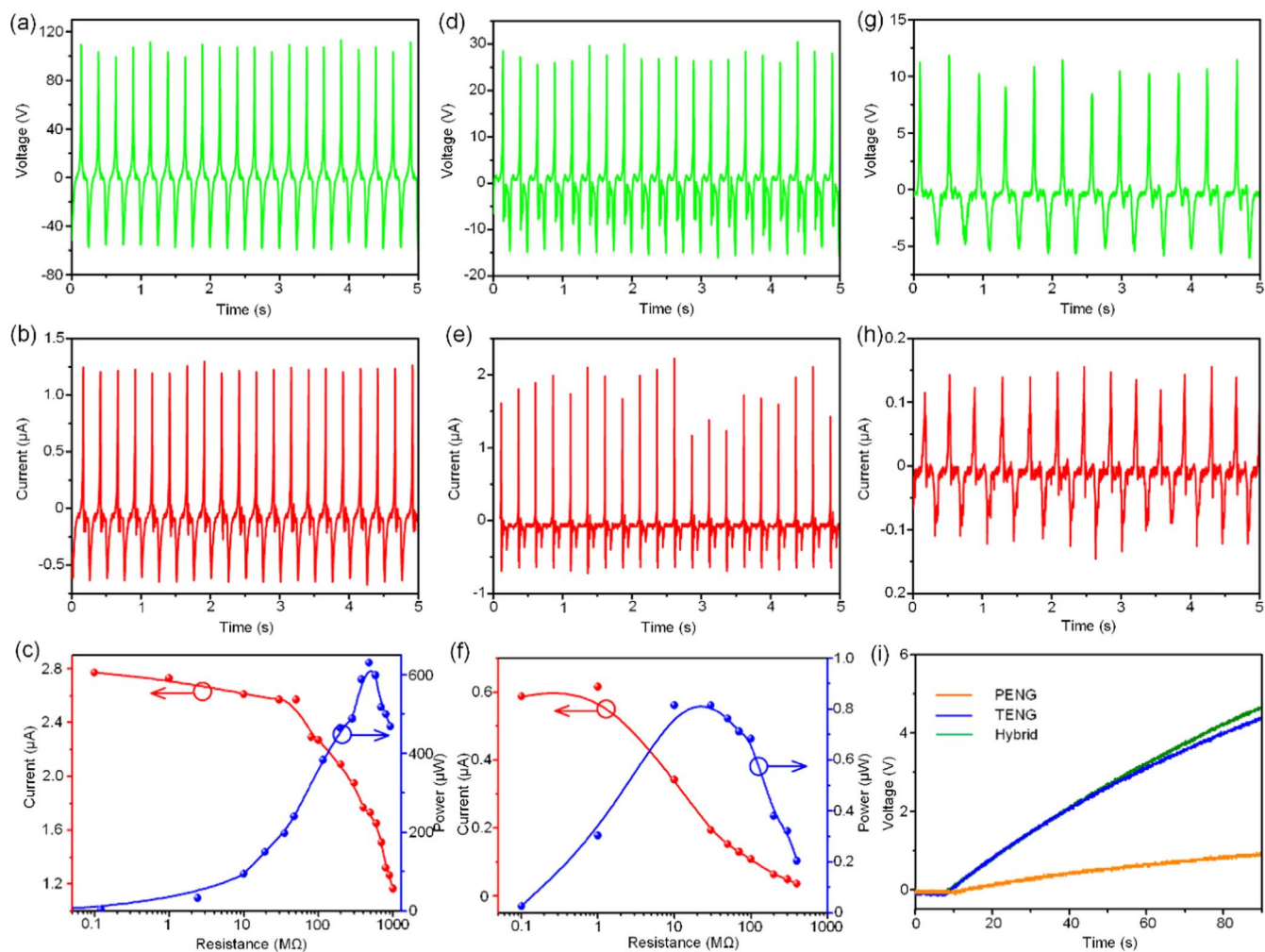


Fig. 3. Electric output of the hybrid NG. (a) The output voltage (b) current (c) and maximum peak power with different resistance load of the TENG. (d) The output voltage (e) current and (f) maximum peak power with different resistance load of the PENG under the press mode. (g) The output voltage and (h) current of the PENG generated from the bend mode. (i) The charging ability of the hybrid NG.

layer between the TENG and PENG electrode is benefit for the output of both part. It worth mentioning that, when the isolation decreased to 0 (i.e. the TENG and PENG part share one electrode), the output for the two-electrode device is much smaller than the sum of the two parts when the isolation exists. This is mainly because that the two electrodes for the PENG part is so close that the electrostatic induction on them induced by the triboelectric charges are almost the same, therefore, weak output can be generated by TENG. Weighing the enhancement of PENG and the whole output performance of the device, it is vital to separate the two parts through a thin isolation layer [41,42].

In real applications, the single electrode TENG can work through contact and separate with other objects while the PENG has two working modes: the pressing (d33) mode and the bending (d31) mode. To quantitatively measure the electric performance under pressing mode, the bottom side of the flexible hybrid NG was anchored and the micro-patterned PDMS side was flapped by cotton cloth that was connected to a vibrator. Fig. 3a presents the measured output voltage of the TENG with a resistance of 100 MΩ at the frequency of 4 Hz, where the peak value reaches 183 V. The measured short-circuit current of the TENG reached 1.96 μA, as displayed in Fig. 3b. Fig. 3c demonstrates the output performance of the nanogenerator under different external loads. Owing to the ohmic loss, the current decrease with increased loading resistance. The output power reaches the peak of 630 μW at a loading resistance of 600 MΩ. Meanwhile, the pressure of the vibrator can also produce piezoelectric output through d33 mode. For the PENG, the output voltage and current were measured to

be 57.1 V and 2.95 μA, respectively, as presented in Fig. 3d and e. Maximum output power of 0.82 μW was obtained at a matched loading resistance of 30 MΩ (Fig. 3f). Besides the pressing mode, the PENG can also generate electricity under the bend deformation. To evaluate the output performance of PENG by the bending mode, we measured its output by folding/unfolding the device at a frequency of about 3 Hz. As shown in Fig. 3f and g, peak voltage of 17.9 V and current of 0.3 μA is generated. Additionally, charging ability of the hybrid NG is also measured and analyzed. In the experiment, a piece of cotton cloth is employed to flap the device at 4 Hz. The generated voltage was then rectified to continuously charge a capacitor of 1 μF. After charging time of 80 s, the capacitor was charged to 0.91 V, 4.35 V and 4.66 V for the PENG part, TENG part and the parallel connection of them, respectively. It should be mentioned that the different charging ability of the two NGs is determined by the amplitude and duration of the output voltage. Under the pressing test mode, the working during time for the TENG is longer than that of PENG, thus the charging ability is much better too.

To investigate the effect of loading pressure on the performance of the hybrid NG, output voltage and current were measured for both parts when the device was applied different strength of force ranging from 5.6 N to 43 N. Notably, the peak voltage and current for the both parts increased proportionally with the increasing applied force, as revealed in Fig S3. It was observed that the voltage raises linearly from ~57 to ~341 V for the TENG while increases from ~7.7 to ~60.1 V for the PENG, corresponding to sensitivity of 7.84 V/N and 1.42 V/N for

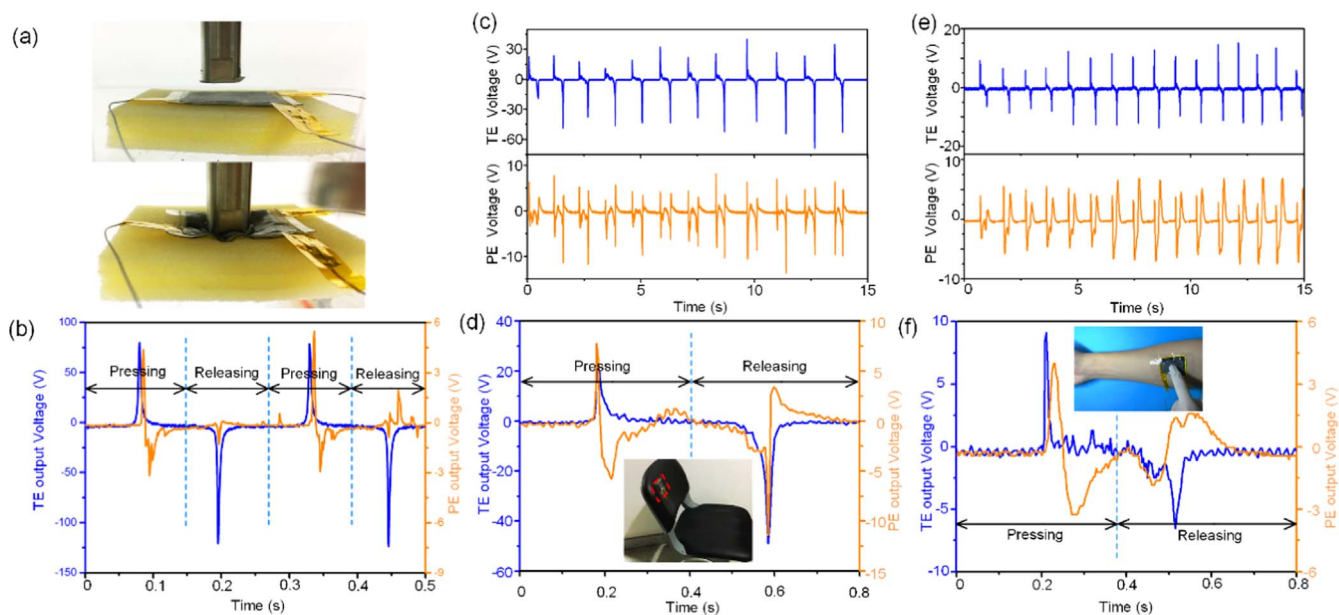


Fig. 4. Application of the hybrid NG for harvesting mechanical energy on soft surface. (a) The test condition of the device for harvesting press energy on soft sponge. (b) The output voltage of the device on soft sponge. (c) Output voltage and (d) the enlarged signal of the hybrid NG on back of chair for harvesting press energy. (e) Output voltage and (f) the enlarged signal when the device is attached on the skin. Insets shows the corresponding photography images for the tests.

the TENG and PENG, respectively. For the current, the sensitivities are $0.106 \mu\text{A/N}$ @ TENG and $0.078 \mu\text{A/N}$ @ PENG, respectively. The linear increase of output for the PENG can be derived from the equation:

$$V_{oc} = T\sigma_{33}g_{33}$$

where T is the thickness of the piezoelectric material, σ_{33} is the stress along the direction of the applied force, g_{33} is the piezoelectric voltage coefficient, respectively. The reason for the linear growth of TENG part can be ascribed to the regular deformation of the micro pyramid structure on the surface of top PDMS [43,44]. The stronger force applied, the larger deformation of the microstructure, thus more tribocharges can be generated on the surface and so does the output. The mechanical deformation simulation of the micro-pyramid structure under applied force is shown in Fig. S4.

3.3. Applications

To verify the validity of the device for harvesting energy on soft surface by both parts through pressing of other objects, the hybrid NG was mounted onto a piece of sponge and tapped by a piece of cotton cloth connected to the vibrator (Fig. 4a). When applied force, the device will be dish into the sponge and generate deformation. Under the continuous tap of 4 Hz, peak voltage of about 200 V for the TENG part and 8 V for the PENG part were obtained, as demonstrated in Fig. 4b. When the cotton contacts with the device, triboelectric output is firstly generated by TENG, then as the pressure continuously increased, piezoelectric material deforms and produces the piezoelectric output. At the releasing process, piezoelectric film recovers to its initial state and generates opposite signal and so does the TENG. Due to the hybrid working characteristic, the device can be mounted on any soft surface for harvesting tapping and pressing energy, for instance, the pressure on back of the chair. The responding voltages as high as 85 V and 10.8 V generated by TENG and PENG are shown in Fig. 4c and d, which are caused by the touch of cloth and the deformation of sponge when people lean on the back. Since human body can produce lots of kinetic energy in daily life, such as the foot press in walking, flapping hands and other behaviors, the device can be attached on the skin to harvest energy of body movements. As shown in Fig. 4e and f, the device is adhered onto an arm and when pressed by finger, both

piezoelectric and triboelectric output can be generated. Different from previous reported generators for body motion energy harvesting, the hybrid NG can not only function where the contact/separation happens, but also work when the pressure changes during continue pressing. When attached on the back of chair, the device can fully contact with the cloth while the deformation of piezoelectric film is relatively small, leading to a large gap between the outputs of TENG and PENG, and the influence of triboelectric charges on the PENG is very obvious. We also demonstrate the device be placed on back of the hand to harvest body motion energy of beating and making a fist, as shown in Fig. S5.

Owing to the high sensitivity of the piezoelectric material, the device can also be attached on different parts of body to for athletes. Here, we demonstrate the flexible hybrid NG adhered on belly for efficient monitoring of human respiratory rate and depth (Fig. 5a). Under varying respiration intensity and frequency, the waveforms generated by the PENG part of the device presents obvious differences, in which each cycle represents one breath, as shown in Fig. 5b. Compared with previously reported self-powered respiratory sensor, the device can be easily attached on skin since it is based on the deformation of piezoelectric film and do not need to be tightly bounded on the body. Moreover, the device is attached to the wrist using medical wristlet acting as a self-powered and noninvasive monitoring for the RAP in real-time. The voltage signals of RAP during 10 s of a 23-year old woman are shown in Fig. 5c and an enlarged view of one cycle is depicted in Fig. 5d (Inset: photograph of the device attached on the wrist). The pulse frequency of 72 beats per min could be read out clearly in the 10 s-monitoring figure, as what is expected for a healthy woman. Four systolic waves and one diastolic wave: initial positive wave (a wave), early negative (b wave), re-increasing (c wave), re-decreasing (d wave) and diastolic (e wave) are clearly shown in the enlarged figure, which contains more information for personal health assessment and clinical diagnosis [45,46].

4. Conclusions

In summary, we have demonstrated a flexible fiber-based hybrid nanogenerator based on electrospinning process with enhanced piezoelectric output. By employing electrospun PU nanofiber mat as a template, highly conductive and stable electrode is fabricated, making

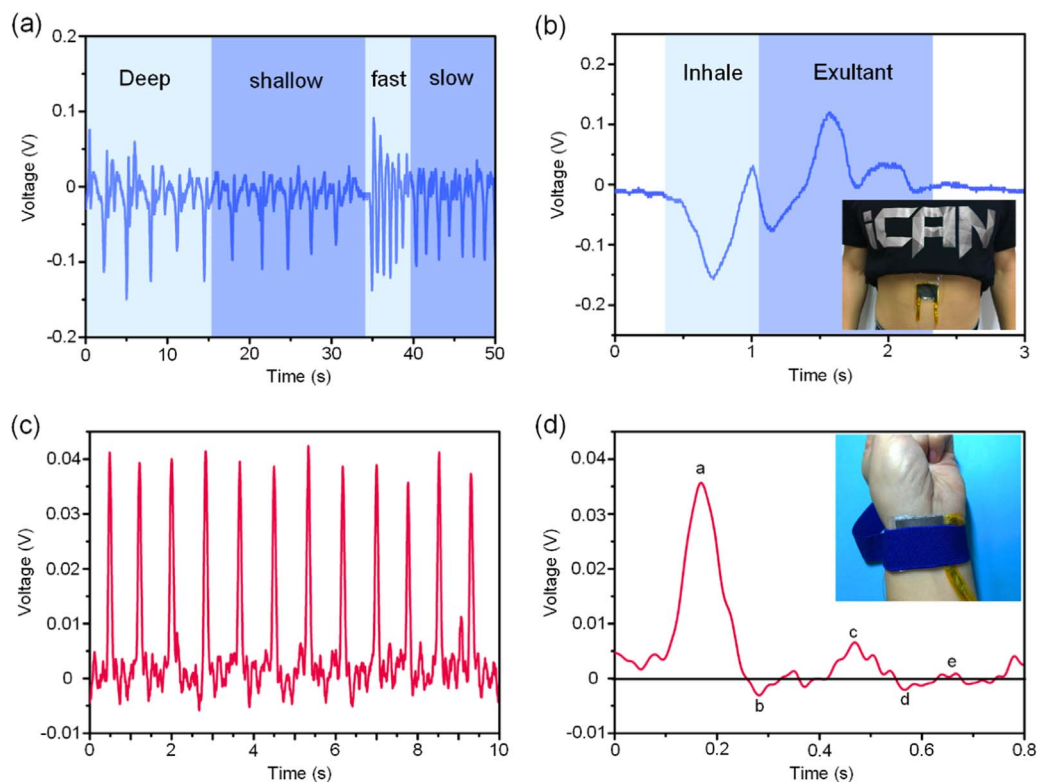


Fig. 5. Hybrid NG for real-time physiological monitoring. (a) Respiratory signal recorded in 50 s with four different breathing states including deep, shallow, fast and slow. (b) The enlarged signal in one breath cycle. (c) The real-time artery pulse signal and (d) the enlarged view of output in one cycle.

the device suitable for harvesting energy on soft surface. Compared with the two electrode hybrid NG, the separate structure design enables the device to generate piezoelectric and triboelectric high outputs simultaneously. When triggered by 4 Hz external force, the output peak voltage, current and power density of the TENG reach 183 V, 1.96 μA and 630 μW , respectively. For the PENG part, the values are 57.1 V, 2.95 μA and 0.85 μW , respectively. The flexible hybrid NG could be easily attached onto the soft surface to harvest the contact-separation or continuous varying pressure energies, such as pressing the foam and body skin, which expands its application range and enhancing energy conversion efficiency. Moreover, by virtue of the high sensitivity of the piezoelectric material, the device can also be used as a self-powered sensor for real-time monitoring human physiological signals such as respiratory information and radial artery pulse, showing its potential applications in wearable healthcare monitoring systems.

Acknowledgements

This work is supported by the National Key Research and Development Program of China (2016YFA0202701), National Natural Science Foundation of China (Grant No. 61674004 and 91323304), and the Beijing Science & Technology Project (Grant No. D151100003315003) and the Beijing Natural Science Foundation of China (Grant No. 4141002).

The authors also want to thank the help from Y.G. Jiang and L.L. Gong of Beihang University, the fabrication of electrospinning nanofibers was carried out at Bionic and Micro/Nano/Bio Manufacturing Technology Research Center in Beihang University.

Appendix A. Supporting information

Supplementary data associated with this article can be found in the online version at doi:10.1016/j.nanoen.2017.05.047.

References

- [1] S.-K. Kang, R.K. Murphy, S.-W. Hwang, S.M. Lee, D.V. Harburg, N.A. Krueger, J. Shin, P. Gamble, H. Cheng, S. Yu, *Nature* 530 (2016) 71–76.
- [2] M. Shi, J. Zhang, H. Chen, M. Han, S.A. Shankaregowda, Z. Su, B. Meng, X. Cheng, H. Zhang, *ACS Nano* 10 (2016) 4083–4091.
- [3] M. Shi, H. Wu, J. Zhang, M. Han, B. Meng, H. Zhang, *Nano Energy* (2017).
- [4] M.K. Choi, J. Yang, K. Kang, D.C. Kim, C. Choi, C. Park, S.J. Kim, S.I. Chae, T.-H. Kim, J.H. Kim, *Nat. Commun.* 6 (2015).
- [5] J.C. Yeo, C.T. Lim, *Microsyst. Nanoeng.* 2 (2016) 16043.
- [6] D. Son, J. Lee, S. Qiao, R. Ghaffari, J. Kim, J.E. Lee, C. Song, S.J. Kim, D.J. Lee, S.W. Jun, *Nat. Nanotechnol.* 9 (2014) 397–404.
- [7] D. Larcher, J.-M. Tarascon, *Nat. Chem.* 7 (2015) 19–29.
- [8] A.R. bin Mohd Yusoff, D. Kim, H.P. Kim, F.K. Shneider, W.J. da Silva, J. Jang, *Energy Environ. Sci.* 8 (2015) 303–316.
- [9] L. Zhang, B. Zhang, J. Chen, L. Jin, W. Deng, J. Tang, H. Zhang, H. Pan, M. Zhu, W. Yang, *Adv. Mater.* 28 (2016) 1650–1656.
- [10] Z. Quan, C.B. Han, T. Jiang, Z.L. Wang, *Adv. Energy Mater.* 6 (2016).
- [11] S. Li, W. Peng, J. Wang, L. Lin, Y. Zi, G. Zhang, Z.L. Wang, *ACS Nano* 10 (2016) 7973–7981.
- [12] X. Cheng, B. Meng, X. Zhang, M. Han, Z. Su, H. Zhang, *Nano Energy* 12 (2015) 19–25.
- [13] J. Wang, S. Li, F. Yi, Y. Zi, J. Lin, X. Wang, Y. Xu, Z.L. Wang, *Nat. Commun.* 7 (2016).
- [14] K. Zhang, X. Wang, Y. Yang, Z.L. Wang, *ACS Nano* 9 (2015) 3521–3529.
- [15] J. Zhong, Y. Zhang, Q. Zhong, Q. Hu, B. Hu, Z.L. Wang, *J. Zhou, ACS Nano* 8 (2014) 6273–6280.
- [16] K. Zhang, Z.L. Wang, Y. Yang, *ACS Nano* 10 (2016) 4728–4734.
- [17] W. Seung, M.K. Gupta, K.Y. Lee, K.-S. Shin, J.-H. Lee, T.Y. Kim, S. Kim, J. Lin, J.H. Kim, S.-W. Kim, *ACS Nano* 9 (2015) 3501–3509.
- [18] Z. Zhao, C. Yan, Z. Liu, X. Fu, L.M. Peng, Y. Hu, Z. Zheng, *Adv. Mater.* 28 (2016) 10267–10274.
- [19] S. Siddiqui, D.-I. Kim, M.T. Nguyen, S. Muhammad, W.-S. Yoon, N.-E. Lee, *Nano Energy* 15 (2015) 177–185.

- [20] M. Zhang, T. Gao, J. Wang, J. Liao, Y. Qiu, Q. Yang, H. Xue, Z. Shi, Y. Zhao, Z. Xiong, *Nano Energy* 13 (2015) 298–305.
- [21] S. Siddiqui, D.-I. Kim, E. Roh, T.Q. Trung, M.T. Nguyen, N.-E. Lee, *Nano Energy* 30 (2016) 434–442.
- [22] X. Cheng, L. Miao, Z. Su, H. Chen, Y. Song, X. Chen, H. Zhang, *Microsyst. Nanoeng.* 3 (2017) 16074.
- [23] Y.C. Lai, J. Deng, S. Niu, W. Peng, C. Wu, R. Liu, Z. Wen, Z.L. Wang, *Adv. Mater.* 28 (2016) 10024–10032.
- [24] X.S. Zhang, M. Su, J. Brugger, B. Kim, *Nano Energy* 33 (2017) 393–401.
- [25] Z.L. Wang, J. Song, *Science* 312 (2006) 242–246.
- [26] K.I. Park, J.H. Son, G.T. Hwang, C.K. Jeong, J. Ryu, M. Koo, I. Choi, S.H. Lee, M. Byun, Z.L. Wang, *Adv. Mater.* 26 (2014) 2514–2520.
- [27] Y. Zi, L. Lin, J. Wang, S. Wang, J. Chen, X. Fan, P.K. Yang, F. Yi, Z.L. Wang, *Adv. Mater.* 27 (2015) 2340–2347.
- [28] Z. Pi, J. Zhang, C. Wen, Z.-B. Zhang, D. Wu, *Nano Energy* 7 (2014) 33–41.
- [29] J. Chang, M. Dommer, C. Chang, L. Lin, *Nano Energy* 1 (2012) 356–371.
- [30] L. Persano, C. Dagdeviren, Y. Su, Y. Zhang, S. Girardo, D. Pisignano, Y. Huang, J.A. Rogers, *Nat. Commun.* 4 (2013) 1633.
- [31] M. Han, X.-S. Zhang, B. Meng, W. Liu, W. Tang, X. Sun, W. Wang, H. Zhang, *ACS Nano* 7 (2013) 8554–8560.
- [32] W.-S. Jung, M.-G. Kang, H.G. Moon, S.-H. Baek, S.-J. Yoon, Z.-L. Wang, S.-W. Kim, C.-Y. Kang, *Sci. Rep.* 5 (2015) 9309.
- [33] X. Chen, M. Han, H. Chen, X. Cheng, Y. Song, Z. Su, Y. Jiang, H. Zhang, *Nanoscale* (2017).
- [34] H. Wu, L. Hu, M.W. Rowell, D. Kong, J.J. Cha, J.R. McDonough, J. Zhu, Y. Yang, M.D. McGehee, Y. Cui, *Nano Lett.* 10 (2010) 4242–4248.
- [35] X.H. Qin, S.Y. Wang, *J. Appl. Polym. Sci.* 102 (2006) 1285–1290.
- [36] W.J. Li, C.T. Laurencin, E.J. Caterson, R.S. Tuan, F.K. Ko, *J. Biomed. Mater. Res.* 60 (2002) 613–621.
- [37] T. Lei, X. Cai, X. Wang, L. Yu, X. Hu, G. Zheng, W. Lv, L. Wang, D. Wu, D. Sun, *RSC Adv.* 3 (2013) 24952–24958.
- [38] A. Baji, Y.-W. Mai, Q. Li, Y. Liu, *Nanoscale* 3 (2011) 3068–3071.
- [39] T.A. Kim, S.-S. Lee, H. Kim, M. Park, *RSC Adv.* 2 (2012) 10717–10724.
- [40] W. Zeng, X.-M. Tao, S. Chen, S. Shang, H.L.W. Chan, S.H. Choy, *Energy Environ. Sci.* 6 (2013) 2631–2638.
- [41] X. Wang, B. Yang, J. Liu, C. Yang, *J. Mater. Chem. A* 5 (2017) 1176–1183.
- [42] H. Li, L. Su, S. Kuang, Y. Fan, Y. Wu, Z.L. Wang, G. Zhu, *Nano Res.* 10 (2017) 1–9.
- [43] J. Zhang, M. Shi, H. Chen, M. Han, Y. Song, X. Cheng, H. Zhang, In ultra-sensitive transparent and stretchable pressure sensor with single electrode, *Micro Electro Mechanical Systems (MEMS)*, in: *Proceedings of the 2016 IEEE 29th International Conference on, IEEE, 2016*; pp 173–176.
- [44] S.C. Mannsfeld, B.C. Tee, R.M. Stoltenberg, C.V.H. Chen, S. Barman, B.V. Muir, A.N. Sokolov, C. Reese, Z. Bao, *Nat. Mater.* 9 (2010) 859–864.
- [45] K. Takazawa, N. Tanaka, M. Fujita, O. Matsuoka, T. Saiki, M. Aikawa, S. Tamura, C. Ibukiyama, *Hypertension* 32 (1998) 365–370.
- [46] B. Wang, C. Liu, Y. Xiao, J. Zhong, W. Li, Y. Cheng, B. Hu, L. Huang, J. Zhou, *Nano Energy* 32 (2017) 42–49.